

Quantum phase transition of two-dimensional NdOCl

Chenfeng Liu(刘晨峰), Wangyang Du(杜汪洋), Fei Gao(高飞), and Hongshuai Tao(陶红帅)
Citation: Chin. Phys. B, 2026, 35 (**8**): 087103. DOI: 10.1088/1674-1056/ae1566
http://cpb.iphy.ac.cn; http://iopscience.iop.org/cpb

What follows is a list of articles you may be interested in

Numerical study of a quantum spin in an s-wave superconductor using the natural orbitals renormalization group method

Wen-Jing Zhang(张文静), Ru Zheng(郑汝), Rong-Qiang He(贺荣强), and Zhong-Yi Lu(卢仲毅)
Chin. Phys. B, 2026, 35 (**2**): 027104. DOI: 10.1088/1674-1056/adf4af

Janus effect of inter-orbital hybridization on correlation strength of strongly correlated systems: A dynamical mean-field study

Jian Sun(孙健), Yinchang Zhao(赵银昌), and Chao Lian(廉超)
Chin. Phys. B, 2026, 35 (**2**): 027103. DOI: 10.1088/1674-1056/adf040

Quantitative determination of the critical points of Mott metal—insulator transition in strongly correlated systems

Yuekun Niu(牛月坤), Yu Ni(倪煜), Jianli Wang(王建利), Leiming Chen(陈雷鸣), Ye Xing(邢晔), Yun Song(宋筠), and Shiping Feng(冯世平)
Chin. Phys. B, 2024, 33 (**1**): 017102. DOI: 10.1088/1674-1056/ad0719

A sport and a pastime: Model design and computation in quantum many-body systems

Gaopei Pan(潘高培), Weilun Jiang(姜伟伦), and Zi Yang Meng(孟子杨)
Chin. Phys. B, 2022, 31 (**12**): 127101. DOI: 10.1088/1674-1056/aca083

Relevance of 3d multiplet structure in nickelate and cuprate superconductors

Mi Jiang(蒋密)
Chin. Phys. B, 2021, 30 (**10**): 107103. DOI: 10.1088/1674-1056/abf646

Quantum phase transition of two-dimensional NdOCl

Chenfeng Liu(刘晨峰)[†], Wangyang Du(杜汪洋)[†], Fei Gao(高飞), and Hongshuai Tao(陶红帅)[‡]

College of Science, Inner Mongolia University of Technology, Hohhot 010051, *China*

(Received 11 July 2025; revised manuscript received 11 October 2025; accepted manuscript online 21 October 2025)

This study employs the cellular dynamical mean-field theory (CDMFT), combined with the continuous-time quantum Monte Carlo (CTQMC) method as the impurity solver, to investigate the metal–Mott insulator phase transition and magnetic phase transition in two-dimensional NdOCl under the interplay of strongly correlated interactions and temperature. By calculating the density of states, double occupancy, Fermi surface, and magnetic order parameters of the system, we demonstrate that second-order phase transitions and magnetic symmetry breaking emerge with increasing interaction strength. These results provide a theoretical and computational basis for the fundamental research and potential applications of two-dimensional structured rare earth metals such as NdOCl, holding significant implications for advancing both basic science and technological developments in correlated quantum materials.

Keywords: strongly correlated systems, quantum phase transition, cellular dynamical mean-field theory, rare earth metals, continuous-time quantum Monte Carlo method

PACS: 71.10.–w, 75.10.Hk, 75.10.–b, 71.10.Fd

DOI: 10.1088/1674-1056/ae1566 **CSTR:** 32038.14.CPB.ae1566

1. Introduction

Phase transitions are mutations that exist widely in nature, typically thermally driven. Unlike classical phase transitions, quantum phase transitions are phenomena caused by quantum fluctuations rather than thermal fluctuations. At ultralow temperatures, where thermal motion is suppressed and systems reside in ground or low-energy excited states, quantum mechanical effects become dominant. Previous studies have elucidated emergent phenomena in condensed matter systems, including rare-earth magnetic insulators and two-dimensional electron gas systems. The unique 4f electronic configuration, strong spin–orbit coupling, and electron correlation effects under low-dimensional confinement in rare-earth-based two-dimensional materials provide an ideal platform for exploring novel quantum phenomena that transcend those of traditional transition-metal two-dimensional materials. In-depth investigation of their quantum phase behavior can not only unveil the coupling mechanisms among charge, spin, and orbital degrees of freedom in low-dimensional, strongly correlated electron systems but may also lead to the discovery of new states of matter, such as quantum spin liquids and unconventional superconducting states, driven by the special f-electron configuration of rare-earth elements, thereby significantly expanding the frontiers of our understanding of low-dimensional quantum materials. On an applied level, novel devices based on the quantum phase transition characteristics of two-dimensional NdOCl possess significant advantages; for example, ultra-low-power switching devices can be constructed by controlling its metal-insulator transition with an electric field, highly sensitive magnetoelectric multifunctional sensors can be realized by leveraging the synergistic effects of magnetic and topological phase transitions, and its unique magnon–exciton coupling phenomena may provide a material basis for developing room-temperature spin quantum bits. These advancements will open new avenues for the development of next-generation low-dimensional spintronics, topological quantum computing, and ultrafast optoelectronic devices, powerfully driving innovative breakthroughs in quantum information technology and high-efficiency electronic devices.

Quantum phase transitions represent an important research direction in condensed matter physics.[1–9] In recent years, various methods have been developed for their study. One such method is dynamical mean-field theory (DMFT), which yields highly accurate results in the center of infinite dimensions.[10–12] However, the central approximation of DMFT is that the self-energy is local and momentum-independent, thereby neglecting non-local spatial correlations and spatial fluctuations in the system. This limitation renders it ineffective in low-dimensional systems. Building upon this foundation, the cellular dynamical mean field theory (CDMFT) emerges as a cluster extension of DMFT.[13–16] As a real-space cluster extension of DMFT, CDMFT systematically incorporates short-range spatial correlations by mapping the lattice problem onto a self-consistently solved cluster impurity model. This simplification reduces the complex many-body problem to a self-consistently solved cluster impurity problem. Building on the work of Chen *et al.*[17] and Jarrell *et al.*,[18] continuous-time quantum Monte Carlo (CTQMC)

[†]These authors contributed equally to this work.

[‡]Corresponding author. E-mail: taohs@imut.edu.cn

© 2026 Chinese Physical Society and IOP Publishing Ltd. All rights, including for text and data mining, AI training, and similar technologies, are reserved.

is employed as the impurity solver in the calculations. This choice enhances the accuracy of the final results. The combination of CDMFT and CTQMC provides valuable insights into the study of phase transitions in two-dimensional NdOCl structures.

2. Model and measurements

In this article, we employ CDMFT and CTQMC to investigate the quantum phase transition in two-dimensional NdOCl. Figure 1(a) shows the atomic structure of two-dimensional NdOCl.[19] In this two-dimensional structure, we select an effective cluster with $N_C = 6$ [see Fig. 1(b)]. Figure 1(c) depicts the first Brillouin zone for the two-dimensional NdOCl lattice. Figure 1(d) shows the density of states near the Fermi surface of oxygen, chlorine, and neodymium atoms in this system when $U/t = 0$. By calculating the single-particle density of states, double occupancy, and Fermi surface, we find that the Nd atom undergoes a phase transition from the metallic state to the Mott insulating state, and we construct the correlation phase diagram.[20,31] This research contributes to a comprehensive understanding of critical phenomena in quantum phase transition systems.

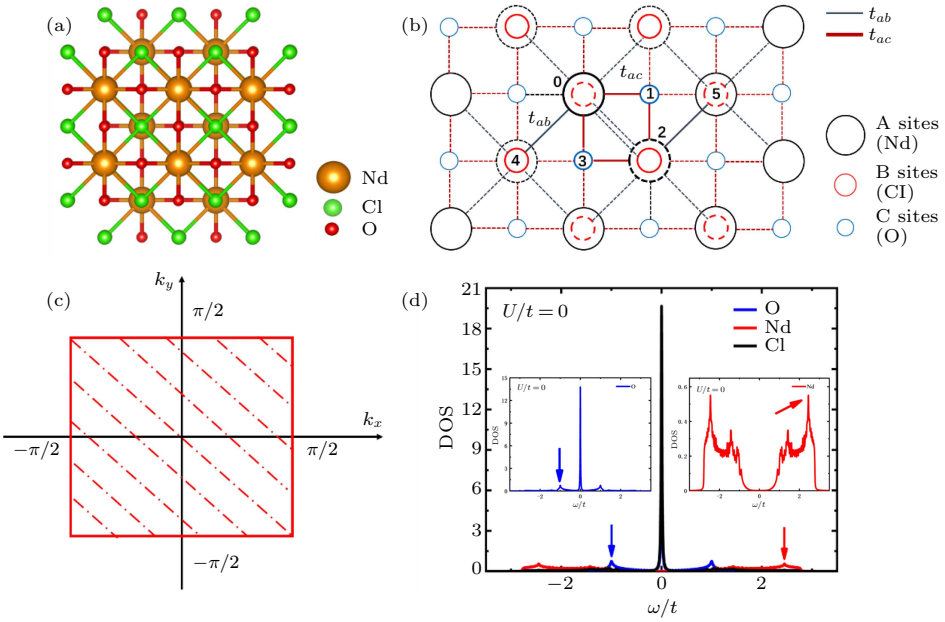


Fig. 1. (a) Atomic structure of two-dimensional NdOCl. (b) Protocell schema ($N_C = 6$). (c) The first Brillouin zone of the unit cluster. (d) Density image of the uninteracted state.

In the study of the quantum phase transition in two-dimensional NdOCl, using the Hubbard model as an example, the Hamiltonian is

$$H = -\sum_{\langle ij\rangle\sigma} t_{ij} c^{\dagger}_{i\sigma} c_{j\sigma} + U\sum_{i} n_{i\downarrow} n_{i\uparrow} + \mu \sum_{i,\sigma} n_{i\sigma}. \tag{1}$$

Here, i and j denote sites in clusters. U is the Coulomb interaction, μ represents the chemical potential, and μ is adjusted to achieve systematic half-filling. $c^{\dagger}_{i\sigma}$ and $c_{i\sigma}$ represent the creation and annihilation operators for fermions with spin σ ($\sigma = 0$ for spin up, $\sigma = 1$ for spin down) at lattice site i. The particle number operator $n_{i\sigma}$ is defined as $n_{i\sigma} = c^{\dagger}_{i\sigma} c_{i\sigma}$. The ratio $\lambda = t_{ab}/t_{ac}$, termed the asymmetry factor, is experimentally tunable through sample compression.[7,21] We use $t = t_{ac} = 1.0$ as the energy unit.

In two-dimensional NdOCl, we select a suitable unit cell as depicted in Fig. 1(b), where the cell configuration fully incorporates quantum fluctuations between adjacent cells and spatial fluctuations within the crystal lattice.

In the case of local self-energy approximation, each lattice point in a many-body system is independent in space, and the whole system is mapped onto the Anderson impurity model. The protocell is taken as an impurity, and the influence of lattice points outside the cell on the protocell is replaced by the Weiss field. The system's behavior, represented by the Hubbard model, can be calculated with the help of the CTQMC method.[22–25] Then, the self-consistent solution is used to calculate the relevant physical quantities, in which the self-consistent calculation needs to provide an initial self-energy (an $N_C \times N_C$ matrix) and use the formula

$$g_0^{-1}(\mathrm{i}\omega) = \left(\sum_{k} \frac{1}{\mathrm{i}\omega + \mu - t(k) - \Sigma(\mathrm{i}\omega)}\right)^{-1} + \Sigma(\mathrm{i}\omega) \tag{2}$$

resulting in Weiss field Green's function $g_0(\mathrm{i}\omega)$, where k is cluster wave vector in the first Brillouin zone, $\hat{t}(k)$ is the hopping matrix defined as $\hat{t}_{ij}(k) = \sum_{r_1 - r_2} t^{r_1 r_2} \mathrm{e}^{-\mathrm{i}k\cdot(r_1 - r_2)}$, with r_1 and r_2 representing the real-space position vectors of grid points. The CTQMC method is selected as the impurity solver.[26–30] By substituting the obtained Green's function into the Dyson equation, the global Green's function $G(\mathrm{i}\omega)$

of the cluster is derived,

$$\sum(\mathrm{i}\omega) = g_0^{-1}(\mathrm{i}\omega) - G^{-1}(\mathrm{i}\omega). \tag{3}$$

The global Green's function of the system is consistent with that of the effective Anderson impurity model.

By applying the Dyson equation $\sum(\mathrm{i}\omega) = g_0^{-1}(\mathrm{i}\omega) - G^{-1}(\mathrm{i}\omega)$, a renormalized self-energy is obtained. The new self-energy is substituted into the global Green's function and iterated through the Dyson equation until convergence. The impurity model's Green's function calculated by CTQMC is then approximated as the lattice Green's function, enabling the computation of physical quantities such as the density of states, double occupancy, and spectral function near the Fermi surface. In this work, the DMFT framework is implemented in C, while the impurity solver utilizes a Monte Carlo open-source package.[32–34] The integration of both components ensures higher computational accuracy.

3. Discussion

The density of states is obtained from the Green's function via analytic continuation, for which we employ the maximum entropy method. The distribution of the density of states of Nd atoms near the Fermi surface at temperatures $T/t = 0.08$ and $T/t = 0.1$ is depicted in Fig. 2. From this figure, it can be seen that the single-particle density of states near the Fermi energy level of the system decreases with the increase of the interaction, regardless of the asymmetry factor $\lambda = 1.0$, $\lambda = 1.25$, or $\lambda = 1.5$, and finally the Mott metal–insulator phase transition occurs at $U = U_C$. As can be seen from this figure, the quasiparticle resonance peaks are observed near the Fermi energy level when the asymmetry factor $\lambda = 1.0$, the temperatures $T/t = 0.08$ and $T/t = 0.1$, and when the interaction is low, such as $U/t = 3.5$. When the interaction increases, the quasiparticle resonance peak splits and a pseudogap appears and eventually opens at the critical values $U_C/t = 5.5$ and $U_C/t = 6.5$. When $\lambda = 1.5$ and $T/t = 0.08$, there is a pseudogap in the system before the Mott metal-insulator phase transition occurs, and the pseudogap opens and the system transforms from a metallic state to an insulating state at $U_C/t = 5.2$. From this figure, it can be seen that when the asymmetry factor is the same, as the temperature increases, the interaction of the system undergoing the phase transition increases, which means that it is more difficult to undergo the Mott metal-insulator phase transition.

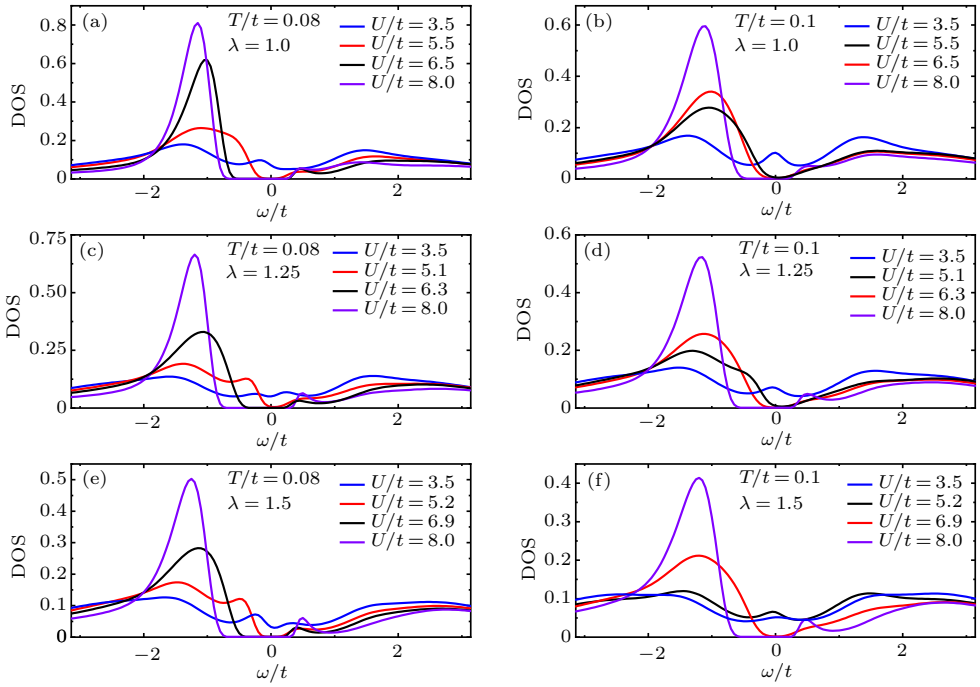


Fig. 2. Density of states of two-dimensional NdOCl. (a) At $T/t = 0.08$ and $\lambda = 1.0$, when the interaction U is stronger than the critical value $U_C/t = 5.5$, the gap near the Fermi energy is opened. (b) At $T/t = 0.1$ and $\lambda = 1.0$, a quasiparticle resonance peak is found before the pseudogap appears. (c) At $T/t = 0.08$ and $\lambda = 1.25$, two-dimensional NdOCl is transformed from metal to Mott insulator at the critical interaction $U_C/t = 5.1$. (d) The density of states for different interaction strengths U at $T/t = 0.1$ and $\lambda = 1.25$. (e), (f) At $\lambda = 1.5$, as the temperature increases, the interaction of the system undergoing the phase transition increases.

The double occupation is introduced to study the phase transition law of the system. Figure 3 mainly depicts the relationship between the double occupation Docc and the interaction U when the system is at different temperatures T. At different temperatures, the double occupation Docc decreases with the increase of the interaction, which is due to the enhancement of Coulomb interaction between electrons on the same lattice point and the suppression of the roving nature of the electrons in the system, and thus the lattice point tends to be single-occupied. The double occupation curve in the fig-

ure is a continuous curve, indicating that the phase transition of the system is a second-order phase transition. The arrows in the figure indicate the critical values of the phase transition at different temperatures. As the temperature T increases, the critical value of the phase transition of the system also increases.

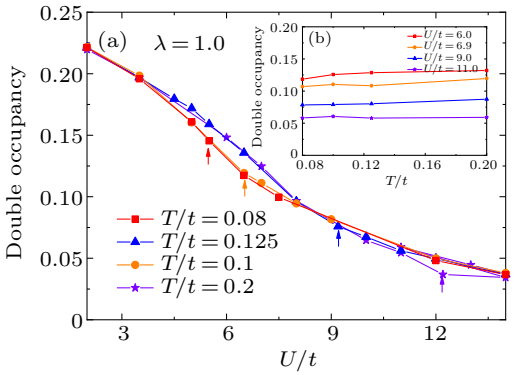


Fig. 3. Double occupancy of two-dimensional NdOCl. (a) The evolution of the double occupancy as a function of on-site repulsive interaction U for different temperatures T. The arrows hint the corresponding value of Mott transition for different temperatures. (b) The value of the double occupancy under certain temperatures for different onsite repulsive interaction U.

We have also studied the magnetic problem on an anisotropic triangular lattice by means of the magnetic order parameter, which is defined as $m = \frac{1}{N_C}\Sigma_i \mathrm{sgn}(i)\left(\langle n_{i\downarrow}\rangle - \langle n_{i\uparrow}\rangle\right)$, where $\mathrm{sgn}(i)$ is the staggering factor required to define the antiferromagnetic order parameter, with $\mathrm{sgn}(i) = 1$ for lattice sites $i = 0$ and 2, and $\mathrm{sgn}(i) = -1$ for the other lattice sites. Figure 4 depicts the asymmetry factor $\lambda = 1.0$ and $T/t = 0.1$ for the system's single-particle energy gap ΔE and staggered magnetization m versus the interaction. When the interaction $U/t < 3.5$, both ΔE and m are 0, indicating that there is no energy gap and the staggered magnetization is 0. The system is in the paramagnetic metallic state. When the interaction $3.5 < U/t < 6.5$, the symmetry of the system is broken, the magnetic order $m \neq 0$, the system is antiferromagnetic, and the single-particle energy gap of the system is still 0, and the system is in the antiferromagnetic metallic state. When the interaction $U/t > 6.5$, the system appears as a single-particle energy gap, and the staggered magnetization $m \neq 0$, the system enters the antiferromagnetic Mott insulating state.

In this paper, the spectral function $A(k, \omega)$ near the Fermi surface of Nd atoms in momentum space is used to simulate the process of the metal–Mott insulator phase transition, as shown in Fig. 5. From the three plots in Fig. 5, it can be seen that the probability of the appearance of particles near the Fermi surface decreases with increasing interaction, the pseudogap near the Fermi surface of the system opens, and the system enters the insulating state. At $U/t = 6.0$, there is a peak in the electron probability density on the Fermi surface, indicating that the system exhibits a metallic state at this point, as shown in Fig. 5(a). The peak near the Fermi surface decreases gradually when the interaction increases to $U/t = 6.9$, as shown in Fig. 5(b). When the interaction is stronger than the critical value of $U/t = 9.0$, the electrons near the Fermi surface are affected by the localization, and the probability of the emergence of particles is extremely low, and at this time the system has entered the insulating state, as shown in Fig. 5(c). The probability of particles appearing on the Fermi surface decreases gradually with increasing interactions at the same temperature, causing the system to undergo a metal–Mott insulator phase transition.

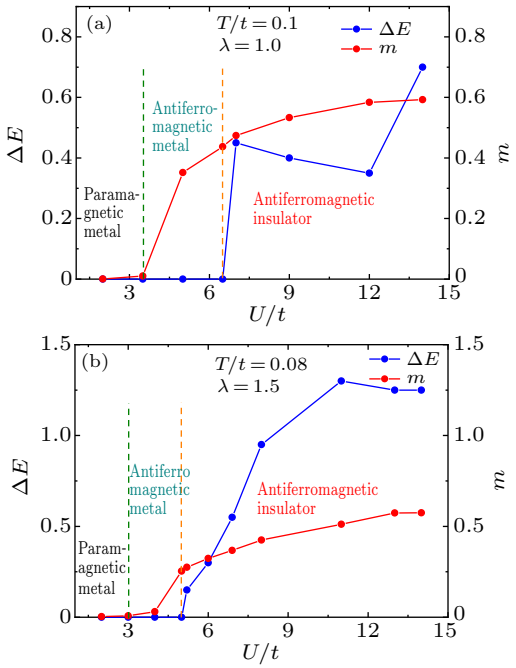


Fig. 4. Relationship between energy gap and the on-site repulsive interaction. (a) The relationship between energy gap and interaction for $T/t = 0.1, \lambda = 1.0$, while (b) for $T/t = 0.08, \lambda = 1.5$.

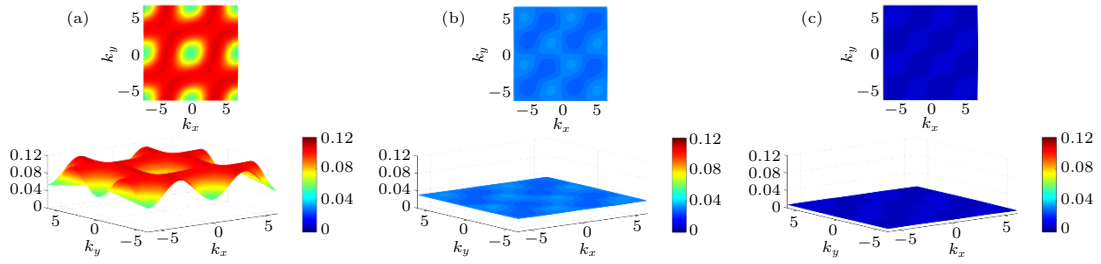


Fig. 5. Fermi surfaces of two-dimensional NdOCl for different interaction strengths at $\lambda = 1.5$ and $T/t = 0.1$. (a) $U/t = 6.0$, (b) $U/t = 6.9$, (c) $U/t = 9.0$.

Combining the previously mentioned single-particle density of states and magnetic order parameter, we finally plotted the quantum phase diagram of two-dimensional NdOCl as a function of λ and U at $T/t = 0.1$ (see Fig. 6).

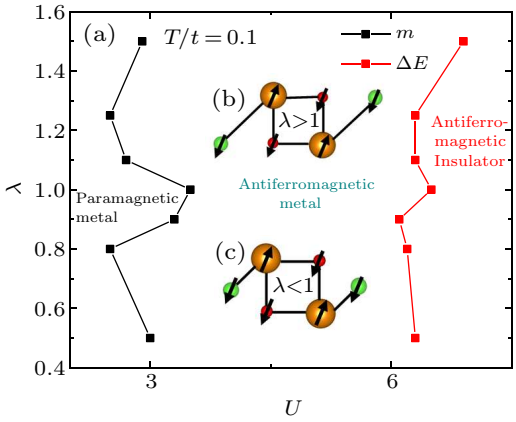


Fig. 6. Phase diagram of the two-dimensional NdOCl representing the competition between U and λ for $T/t = 0.1$.

4. Conclusion

In this paper, we have investigated the process of the metal–Mott insulator phase transition of two-dimensional NdOCl using a combination of CDMFT and CTQMC, and found that only the Nd atoms in the structure undergo a quantum phase transition when the temperature T and the interaction U reach a critical value, whereas a large number of itinerant electrons appear in the O and Cl atoms, which makes a sharp Fermi liquid-like peak always near the Fermi surface. Under the change of interaction U, the local electrons in the system are dominant and the roaming electrons are suppressed, making the electrons in the lattice sites tend to be single-occupied, resulting in a continuously decreasing double occupancy change curve, which indicates that the phase transition occurring in this structure is a second-order phase transition.

Acknowledgements

This work was supported by the National Natural Science Foundation of China (Grant No. 11805105), the Natural Science Foundation of Inner Mongolia Autonomous Region of China (Grant No. 2018LH01010), and the Program for Young Talents of Science and Technology in Universities of Inner Mongolia Autonomous Region of China (Grant No. NJYT-20-B11).

References

[1] Brody D C, Hugheston L P and Parry M F 2010 *Phys. Lett. A* **374** 2424
[2] Tiwari R and Majumdar P 2012 *Curr. Sci.* **103** 518
[3] Zhang T F, Li C X and Liu W M 2023 *Chin. Phys. B* **32** 090501
[4] Wu H, Ma Z, Jiang Y, Wang L, Yang H, Li Y, Zuo P, Jia H, Wang W, Zhou J, Liu W and Chen H 2016 *Chin. Phys. B* **25** 117803
[5] Ramakrishnan T V 2008 *Curr. Sci.* **95** 1284
[6] Aryanpour K, Maier T A and Jarrell M 2005 *Phys. Rev. B* **71** 037101
[7] Chen Y H, Wu W, Tao H S and Liu W M 2010 *Phys. Rev. A* **82** 043625
[8] Lin H F, Tao H S, Guo W X and Liu W M 2015 *Chin. Phys. B* **24** 057101
[9] Gao Y, Zhang M, Fu M, Hu W, Tong H and Tao Z 2023 *Energy Rev.* **2** 100038
[10] You B L, Liu X Y, Cheng S J, Wang C and Gao X L 2021 *Acta Phys. Sin.* **70** 100201 (in Chinese)
[11] Jarrell M, Macridin A, Mikelsons K, Doluweera D G S P, Gubernatis J E, Avella A and Mancini F 2008 *AIP Conf. Proc.* **1014** 34
[12] Coulamy I B, Warnes J H, Sarandy M S and Saguia A 2016 *Phys. Lett. A* **380** 1724
[13] Li L, Wang C H, Yin H H, Wang R Q and Liu W M 2024 *Chin. Phys. B* **33** 020306
[14] Pavlov V A and Zlotin S G 2018 *Curr. Org. Chem.* **22** 2029
[15] Vojta M 2003 *Rep. Prog. Phys.* **66** 2069
[16] Ahami N, Azzouz M and El Baz M 2024 *Phys. Lett. A* **523** 129770
[17] Go A and Jeon G S 2009 *J. Phys. Condens Matter* **21** 485602
[18] Imada M, Fujimori A and Tokura Y 1998 *Rev. Mod. Phys.* **70** 1039
[19] Verret S, Roy J, Foley A, Charlebois M, Sénéchal D and Tremblay A M S 2019 *Phys. Rev. B* **100** 224520
[20] Liu H, Bao J, Yan H and Guo B 2024 *Phys. Lett. A* **526** 129955
[21] Wang B, Li K, Liu J, Zhang T, Yang T and Zhang N 2024 *Int. J. Hydrogen Energy* **61** 216
[22] Müller-Hartmann E 1989 *Z. Phys. B Condens Matter* **76** 211
[23] Bao A, Tao H S, Liu H D, Zhang X and Liu W M 2014 *Sci. Rep.* **4** 6918
[24] Maier T, Jarrell M, Pruschke T and Hettler M H 2004 *Rev. Mod. Phys.* **77** 1027
[25] Kennedy W, Sousa-Júnior S D, Costa N C and dos Santos R R 2022 *Phys. Rev. B* **106** 165121
[26] Affleck I and Marston J B 1988 *Phys. Rev. B* **37** 3774
[27] Chen Y H, Tao H S, Yao D X and Liu W M 2012 *Phys. Rev. Lett.* **108** 246402
[28] Wu W, Chen Y H, Tao H S and Liu W M 2010 *Phys. Rev. B* **82** 245102
[29] Sørensen A S, Demler E, Lukin M D 2005 *Phys. Rev. Lett.* **94** 086803
[30] Georges A, Kotliar G, Krauth W and Rozenberg M J 1996 *Rev. Mod. Phys.* **68** 13
[31] Kim S and Lee H 2017 *J. Korean Phys. Soc.* **70** 1049
[32] Biroli G and Kotliar G 2002 *Phys. Rev. B* **65** 155112
[33] Parcollet O, Biroli G and Kotliar G 2004 *Phys. Rev. Lett.* **92** 226402
[34] Si Q and Steglich F 2010 *Science* **329** 1161